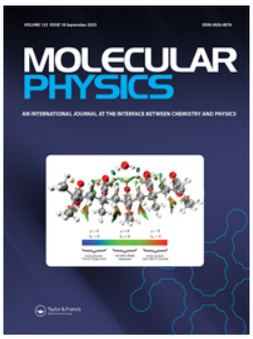

Taylor & Francis
Taylor & Francis Group

Molecular Physics

An International Journal at the Interface Between Chemistry and Physics

ISSN: 0026-8976 (Print) 1362-3028 (Online) Journal homepage: www.tandfonline.com/journals/tmph20

MARVEL analysis of high-resolution rovibrational spectra of $^{16}O^{13}C^{17}O$ and $^{17}O^{12}C^{17}O$

Malak H. I. Mansour, Aisha B. I. Al-Iter, Ala'a A. A. Azzam, Jonathan Tennyson, Tibor Furtenbacher & Attila G. Császár

To cite this article: Malak H. I. Mansour, Aisha B. I. Al-Iter, Ala'a A. A. Azzam, Jonathan Tennyson, Tibor Furtenbacher & Attila G. Császár (04 Sep 2025): MARVEL analysis of high-resolution rovibrational spectra of $^{16}O^{13}C^{17}O$ and $^{17}O^{12}C^{17}O$, Molecular Physics, DOI: 10.1080/00268976.2025.2550568

To link to this article: https://doi.org/10.1080/00268976.2025.2550568

MOLECULAR PHYSICS e2550568
https://doi.org/10.1080/00268976.2025.2550568

Taylor & Francis
Taylor & Francis Group

FESTSCHRIFT IN HONOUR OF ZLATKO BACIC

MARVEL analysis of high-resolution rovibrational spectra of $^{16}O^{13}C^{17}O$ and $^{17}O^{12}C^{17}O$

Malak H. I. Mansour [a], Aisha B. I. Al-Iter [a], Ala'a A. A. Azzam [b], Jonathan Tennyson [c], Tibor Furtenbacher [d] and Attila G. Császár [d]

[a]Research Department, AstroJo Institute, Amman, Jordan; [b]Department of Physics, The University of Jordan, Amman, Jordan; [c]Department of Physics and Astronomy, University College London, London, UK; [d]Institute of Chemistry, ELTE Eötvös Loránd University, Budapest, Hungary

ABSTRACT

Spectroscopic networks (SN) are assembled for the carbon dioxide (CO_2) isotopologues $^{16}O^{13}C^{17}O/^{17}O^{12}C^{17}O$ (637/727, according to a well-established shorthand notation adopted in this study), based on line-centre measurements listed in 19/16 literature studies. For the isotopologues 637/727, the SNs contain 5053(3099)/10,256(6657) measured(unique) transitions, determining 18/38 vibrational band origins, defined as the lowest-energy state for a set of vibrational quantum numbers. The transitions collected span the wavenumber regions 617–8061/582–12,570 cm^{-1} for 637/727. These SNs determine 1960/3278 empirical rovibrational energy levels for 637/727, extracted with the help of the MARVEL (Measured Active Rotational-Vibrational Energy Levels) protocol and code. The energy levels of 637/727 span the regions 0–9210/0–13,199 hc cm^{-1} and the polyad numbers P from 0–12 for 637 and from 0–11 and 17 for 727 (where $P = 2v_1 + v_2 + 3v_3$, and the quantum numbers v_1, v_2, and v_3 represent the symmetric stretch, bend, and antisymmetric stretch motions). Comparison of the empirical rovibrational energy levels determined in this study with their counterparts in two published databases, CDSD-296 and Ames-2021, shows very good overall agreement.

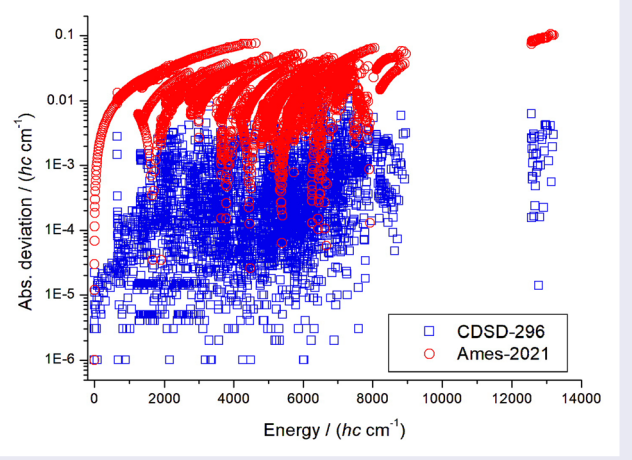

ARTICLE HISTORY
Received 12 March 2025
Accepted 17 August 2025

KEYWORDS
Rovibrational energy levels; CO_2; line positions; transitions; MARVEL

1. Introduction

The present study deals with a network-theoretical investigation of the measured high-resolution (rotational-vibrational) spectroscopy of two minor, doubly-substituted isotopologues of carbon dioxide (CO_2), $^{16}O^{13}C^{17}O$ and $^{17}O^{12}C^{17}O$. $^{16}O^{13}C^{17}O$ and $^{17}O^{12}C^{17}O$ are the sixth and ninth most abundant isotopologues of carbon dioxide, with natural abundances of 8.246×10^{-6} and 1.370×10^{-7}, respectively (see Table 1 for the natural abundances of these and further carbon dioxide isotopologues in the Earth's atmosphere). This study is part of our longer-term project aimed at the determination

CONTACT Ala'a A. A. Azzam alaa.azzam@ju.edu.jo Department of Physics, The University of Jordan, Queen Rania St, Amman, Jordan; Jonathan Tennyson j.tennyson@ucl.ac.uk Department of Physics and Astronomy, University College London, Gower Street, London WC1E 6BT, UK

Supplemental data for this article can be accessed online at http://dx.doi.org/10.1080/00268976.2025.2550568.

Table 1. The number of empirical (MARVEL) rovibrational energy levels determined by our groups for isotopologues of carbon dioxide, and the maximum absolute (MAD) and average absolute (AAD) energy level differences, ΔE, in $hc\,\mathrm{cm}^{-1}$, between our MARVEL studies [1–7] and those from Ames-2021 [8] and CDSD-296 [9]. Nat.abund. = natural abundance.

Isotopologue	Nat. abund.	No. of levels	$\Delta E^{\mathrm{MAD}}_{\mathrm{Ames-2021}}$	$\Delta E^{\mathrm{AAD}}_{\mathrm{Ames-2021}}$	$\Delta E^{\mathrm{MAD}}_{\mathrm{CDSD-296}}$	$\Delta E^{\mathrm{AAD}}_{\mathrm{CDSD-296}}$
$^{16}O^{12}C^{16}O$ (626) [1]	9.842×10^{-1}	8268	0.147	0.015	0.077	0.001
$^{16}O^{13}C^{16}O$ (636) [2]	1.105×10^{-2}	6318	0.152	0.016	0.081	0.002
$^{16}O^{12}C^{18}O$ (628) [3]	3.947×10^{-3}	8786	0.231	0.022	0.182	0.002
$^{16}O^{12}C^{17}O$ (627) [4]	7.339×10^{-4}	5036	0.085	0.012	0.009	0.001
$^{16}O^{13}C^{18}O$ (638) [5]	4.434×10^{-5}	3975	0.151	0.024	0.268	0.002
$^{16}O^{13}C^{17}O$ (637) [this work]	8.246×10^{-6}	1960	0.087	0.014	0.033	0.001
$^{18}O^{12}C^{18}O$ (828) [6]	3.957×10^{-6}	3923	0.571	0.042	0.559	0.002
$^{17}O^{12}C^{18}O$ (728) [6]	1.472×10^{-6}	4318	0.109	0.024	0.046	0.001
$^{17}O^{12}C^{17}O$ (727) [this work]	1.370×10^{-7}	3278	0.105	0.017	0.017	0.001
$^{18}O^{13}C^{18}O$ (838) [6]	4.400×10^{-8}	1058	0.168	0.045	0.039	0.001
$^{17}O^{13}C^{18}O$ (738) [7]	1.700×10^{-8}	945	0.123	0.029	0.014	0.001
$^{17}O^{13}C^{17}O$ (737) [7]	2.000×10^{-9}	877	0.071	0.018	0.008	0.001

of the largest possible sets of empirical rovibrational energy levels for all isotopic variants of the carbon dioxide molecule, involving ^{12}C, ^{13}C, ^{16}O, ^{17}O, and ^{18}O, based on all the available experimental information. Following a well-established shorthand notation introduced within the HITRAN project [10], it is usual to denote the isotopologues of carbon dioxide by a symbol containing three numbers, one for each atom indicative of its mass; for example, the shorthand symbol of the parent carbon dioxide isotopologue, $^{16}O^{12}C^{16}O$, is 626. Empirical rovibrational energy levels have already been published by the groups participating in this project for the carbon dioxide isotopologues 626 [1], 636 [2], 628 [3], 627 [4], 638 [5], 838 [6], 728 [6], 828 [6], 738 [7], and 737 [7] (see Table 1 for a brief overview of some of the important characteristics of these published studies).

Whether the aim is to study the radiative balance of the Earth's atmosphere to appreciate the impact of rising CO_2 levels [11], to explore the atmosphere of neighbouring planets like Venus and Mars [12], or to investigate the atmospheres of exoplanets [13], the spectra of carbon dioxide provide valuable information. Over the last half of a century, a large number of experimental high-resolution spectroscopic studies have been published for both the 637 [14–33] and 727 [12, 24–26, 28, 29, 33–41] isotopologues of carbon dioxide. Not all of these studies report new line position measurements; thus, not all of them have been utilised during this study (see Section 2.5). The experimental line positions, taken from the cited references, are analysed with the help of the MARVEL protocol [42–47], leading to empirical rovibrational energy levels from the validated transitions. The validated experimental rovibrational transitions and the empirical energy levels they determine are the principal results of this study.

Due to the importance of accurate high-resolution spectroscopic data related to isotopologues of carbon dioxide, they are available in several line-by-line spectroscopic databases, such as, in alphabetical order, the Carbon Dioxide Spectroscopic Databank (CDSD-296) [9], ExoMol [48], HITRAN 2020 [10], and NASA Ames-2021 [8]. It is not a simple task to go beyond what is available in these databases. Nevertheless, concentrating on the measured spectra, as done in this study, and completing a global analysis of the measured transitions, provides new information and helps to discover possible errors in the experimental data collected, such as incorrect line-centre positions and assignments. It is expected that the data obtained in this study will enhance spectroscopic line-by-line databases, such as HITRAN [10] and ExoMol [48, 49], and contribute to the refinement of theoretical and computational spectroscopic models.

During studies of the high-resolution spectroscopy of isotopologues of carbon dioxide, understanding the distinctions between the symmetric and asymmetric species is important, as different selection rules apply for the symmetric isotopologues, such as $^{17}O^{12}C^{17}O$ (727), and the asymmetric isotopologues, such as $^{16}O^{13}C^{17}O$ (637). The spectra of the symmetric species are somewhat simpler, since asymmetry relaxes some selection rules and in principle leads to further lines in the rovibrational spectra.

2. Theoretical background

2.1. MARVEL

MARVEL [42–47] is basically a tool which can be used to (a) efficiently analyze and validate assigned line-centre positions determined in high-resolution spectra, and (b) determine empirical energy levels from the validated transitions. It works through the construction of a 'spectroscopic network' (SN) [50, 51], where the energy levels are the vertices and the transitions between them are the edges. When experimentally measured transitions

are collected for a MARVEL analysis, one must ensure that each line has an accurate centre position with an associated uncertainty (the uncertainties of our input datasets are interpreted as expanded uncertainties with coverage factor $k = 2$, roughly corresponding to a 95% confidence interval), and that the upper and lower energy levels involved in the transition are labelled uniquely (see Section 2.2).

The SN of 727 contains two principal components, *para*- and *ortho*-$^{17}O^{12}C^{17}O$. Since no transition between members of the *ortho* and *para* components is allowed, the energy difference between their lowest energies (the so-called roots of the components) must be determined using external information. In this study, this energy difference comes from an effective Hamiltonian given by 86BrSoFr [52]. In cases where the experimentally measured information is highly incomplete, the spectroscopic network may become fragmented, leaving some energy levels isolated from the component(s) containing the root(s) of the SN. These so-called 'floating components' can be connected to the principal components and the measured transitions using sufficiently accurate empirical data (coming from perhaps effective Hamiltonian fits) or, for some molecules, by using the known quasi-degeneracy of certain energy levels [53].

Unlike quantum-chemical models based on the nuclear Hamiltonian, culminating in the solution of the corresponding nuclear Schrödinger equation with approximate potential energy surfaces [54], the accuracy of the empirical (MARVEL) energy levels is not restricted by assumptions other than the validity of the Ritz principle [55] and, of course, the accuracy of the measured line-centre positions. This allows maintaining experimental accuracy during a MARVEL analysis. A caveat is that it also allows MARVEL to accept transitions that might break standard selection rules or are incorrect otherwise, as long as the transition is not in conflict with the other entries of the dataset.

In this study, we used the latest version of the MARVEL code, `MARVEL4` [47]. `MARVEL4` has the option to use an adaptation of the bootstrap method to give final uncertainties for the energy levels; our final energy levels are given with uncertainties obtained using this procedure.

2.2. Notation and quantum numbers

There are two ways to assign quantum numbers to the vibrational states of the linear CO_2 molecule. The first is the Herzberg notation, which is based on the harmonic oscillator model. This uses four quantum numbers: $(\tilde{\nu}_1, \tilde{\nu}_2^{\tilde{\ell}_2}, \tilde{\nu}_3)$. Here, $\tilde{\nu}_1$ represents the symmetric stretching of the molecule, $\tilde{\nu}_2$ refers to the bending, and $\tilde{\nu}_3$ represents the antisymmetric stretching. The $\tilde{\ell}_2$ value describes the angular momentum related to the bending mode and can take values of $\tilde{\nu}_2, \tilde{\nu}_2 - 2, \tilde{\nu}_2 - 4$, and so on, down to 1 or 0. The interaction between the ν_1 and $2\nu_2$ states of CO_2 (known as Fermi resonance) led to a second notation called AFGL (Air Force Geophysics Laboratory) [56–60]. This notation is what we use here. There is no clear way to convert between Herzberg and AFGL, so we combined data from several sources to match the Herzberg notation to AFGL.

The AFGL notation groups the vibrational states into Fermi polyads and uses five vibrational quantum numbers, $(\nu_1\nu_2\ell_2\nu_3 r)$, where r is the Fermi-resonance ranking index (the index r is used to distinguish the levels belonging to the same Fermi polyad). In this notation, the Fermi polyads are determined by ν_1, ℓ_2, and ν_3 [61]; ν_2 is always equal to ℓ_2, and r takes values from 1 to $\nu_1 + 1$. The lowest value of r, 1, is assigned to the energy level with the highest wavenumber (or frequency), and r increases for lower energy levels.

The polyad number P is not a quantum number, but it behaves similarly to one. For carbon dioxide, using the approximate relationships between the harmonic frequencies, $\omega_1 \approx 2\omega_2$ and $\omega_3 \approx 3\omega_2$, the commonly accepted definition of P, which is also employed in this study, is $P = 2\nu_1 + \nu_2 + 3\nu_3$ (see Figure 1 for the distribution of the P values as a function of the energy level for the two carbon dioxide isotopologues studied).

The quantum number J represents the angular momentum associated with the rotational and, when $\ell_2 > 0$, vibrational motion of the CO_2 molecule. Transitions with $\Delta J = -1$ and $\Delta J = +1$ are referred to as P- and R-branch transitions, respectively, while the Q-branch transitions correspond to $\Delta J = 0$. Both P and R transitions occur in the parallel and perpendicular bands, whereas Q-branch transitions are restricted to the perpendicular bands. The 'direction' here refers to the change in the dipole moment driving the transition relative to the linear equilibrium structure of the molecule. For states with $\ell_2 = 0$ the rotationless parity is 'e', while for nonzero ℓ_2 values it can be both 'e' and 'f'. The coupling between rotational and vibrational angular momenta implies that $J \geq l_2$.

The upper and lower states involved in a transition are denoted as $'$ and $''$, respectively. The P, R, and Q transitions are typically identified by the rotational quantum number of the lower state (J''). For the MARVEL analysis, each state is uniquely defined by a set of seven descriptors: $(J\ \nu_1\ \nu_2\ \ell_2\ \nu_3\ r\ e/f)$. This format is also used for the data presented in the Supplementary Material accompanying this paper.

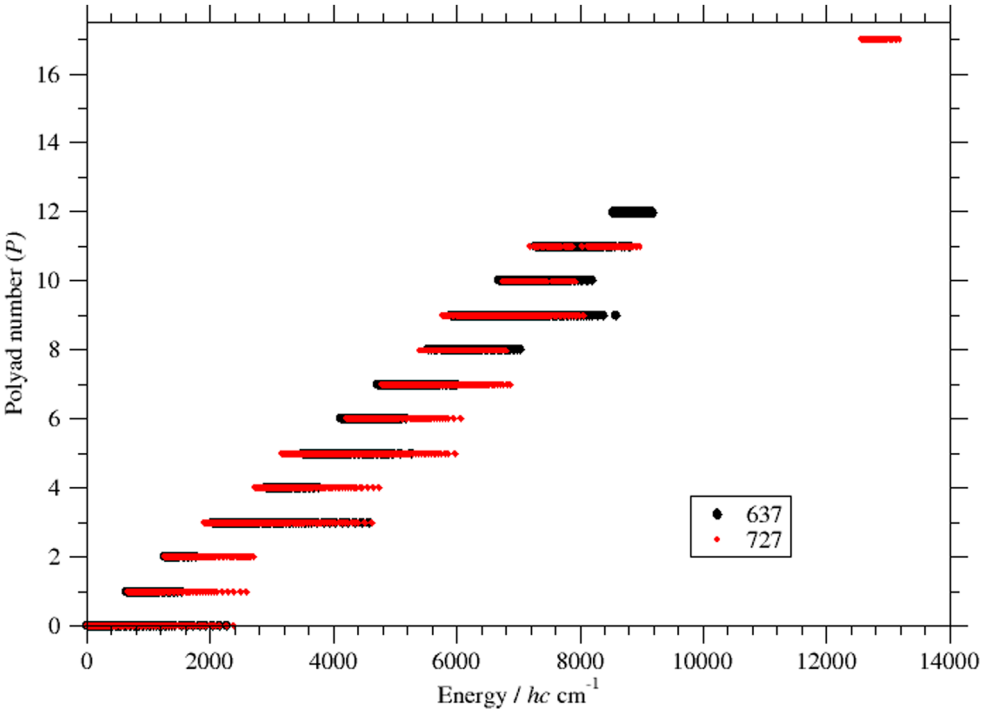

Figure 1. The polyad number, $P = 2v_1 + v_2 + 3v_3$, for each empirical energy level versus the energy levels calculated using MARVEL for the $^{16}O^{13}C^{17}O$ (637, black dots) and $^{17}O^{12}C^{17}O$ (727, red dots) isotopologues of carbon dioxide.

2.3. Selection rules

Toward building a self-consistent dataset during our MARVEL analysis, we tested the spectroscopic data collected for incorrectly labelled transitions. As part of this procedure, fulfilment of the appropriate dipole selection rules and the violation of the *ortho*/*para* selection rule, in the case of 727, were checked. For the 637 and 727 isotopologues, the rovibrational selection rules [61] are $\Delta J = -1, 0, +1$, and if $\Delta J = \pm 1$, then $e \leftrightarrow e$ and $f \leftrightarrow f$ are the allowed transitions, while if $\Delta J = 0$, then $e \leftrightarrow f$ is allowed, but $J = 0 \not\leftrightarrow 0$.

^{17}O has non-zero nuclear spin. Thus, unlike the case of 626, all rotation-vibration levels exist both for 637 and 727. Furthermore, in the case of 727, there are two nuclear spin isomers, conventionally called *para* and *ortho*. If one uses p to denote e and f states with $p = 0$ for e and $p = 1$ for f, then the *ortho* and *para* states are defined by $(J + v_3 + \ell_2 + p)$ being odd and even, respectively. Transitions between *ortho* and *para* states can occur through hyperfine interactions [62]; nevertheless, such transitions are very weak and have not been observed for any isotopologue of CO_2. In principle, there is no such strict constraint on the rovibrational transitions of 637; but, in practice, only relatively few transitions corresponding to *ortho-para* changing have been observed, they form only about 10% of the total number of observed transitions of 637, the rest are *para-para* and *ortho-ortho* transitions.

2.4. Comments on the literature sources used

Table 2 contains details about the data sources treated during the present study for $^{16}O^{13}C^{17}O$ and $^{17}O^{12}C^{17}O$. In particular, Table 2 provides information about the number of assigned (A), floating (F), validated (V), and deleted (D) transitions.

The total number of rovibrational transitions measured for 637/727 is 5053/10,256, including 3099/6657 unique ones, collected from 19/16 experimental sources. As seen for the significantly smaller number of unique transitions compared to all the measured ones, there are a large number of measurements defining multiple edges for the spectroscopic networks of 637 and 727. The most frequently measured transition of the 637 isotopologue is the (1 0 0 0 1 1 e) ← (2 0 0 0 0 1 e) one, which has been measured four times [15, 17, 18, 24]. As to the 727 molecule, the transition (0 3 0 0 1 3 e) ← (1 0 0 0 0 1 e) has been measured five times [24, 26, 37, 41, 63]. In contrast, there are 1681 and 4057 transitions which were measured only once for 637 and 727, respectively.

According to Table 2, 4903/10,145 transitions could be validated for 637/727. For 637, we did not need to delete any of the measured transitions. In the case of 727, we had to delete the following 90 measured transitions: 70 lines from the source 12VaKaHe [63] and 20 from 11VaKaHe [37]. All the deleted 727 transitions belong to the following vibrational bands: (J' 3 1 1 1 2 e/f) ← (J'' 0 1 1 0 0 e/f), (J' 3 1 1 1 3 e/f) ← (J'' 0 1 1 0 1 e/f), and (J' 3 1 1

Table 2. $^{16}O^{13}C^{17}O$ and $^{17}O^{12}C^{17}O$ data sources treated during the present study and some of their characteristics, including the number of measured (A), floating (F), validated (V), and deleted (D) transitions. U^{CS} is the average expanded 'claimed source' uncertainty, and U^{MS} is the average expanded 'MARVEL-suggested' uncertainty.

Isotopologue	Source	Range/cm^{-1}	$A/F/V/D$	U^{CS}	U^{MS}
$^{16}O^{13}C^{17}O$	98TeClVa [18]	617.52–2305.02	94/0/94/0	2.5×10^{-4}	2.7×10^{-4}
(637)	85Jolma [16]	618.25–675.04	64/0/64/0	5.0×10^{-4}	5.7×10^{-4}
	12LyKaJaLu [24]	1977.04–4983.91	860/42/818/0	1.1×10^{-3}	1.2×10^{-3}
	86EsSaRoVa [17]	2203.91–2316.09	99/5/94/0	2.0×10^{-3}	2.2×10^{-3}
	78BaLiDeRa [15]	2229.25–2297.51	60/0/60/0	2.5×10^{-3}	3.4×10^{-3}
	14BoJaLyTa [25]	3423.86–4545.12	673/68/605/0	3.3×10^{-4}	4.1×10^{-4}
	04DiMaRoPe [19]	4489.24–6768.64	595/0/595/0	1.2×10^{-3}	1.4×10^{-3}
	15BoJaLyTa [28]	4681.88–4878.49	158/0/158/0	2.3×10^{-4}	3.9×10^{-4}
	19MoKaPeTa [33]	5696.34–5849.92	152/0/152/0	1.0×10^{-3}	1.1×10^{-3}
	18KaSiCeMo [32]	5702.17–5850.46	147/0/147/0	1.0×10^{-3}	1.1×10^{-3}
	18KaCeMoKa [30]	5703.30–5850.46	62/0/62/0	1.0×10^{-3}	1.1×10^{-3}
	18CeKaMoKa [31]	5810.89–5828.13	11/0/11/0	1.0×10^{-3}	1.6×10^{-3}
	08PePeCa [22]	5875.05–6768.64	992/32/960/0	1.0×10^{-3}	1.2×10^{-3}
	06PeKaRoPe [20]	6005.79–6768.64	249/2/247/0	2.0×10^{-3}	2.1×10^{-3}
	14KaCaMoKa [26]	6044.51–6768.64	335/0/335/0	1.0×10^{-3}	1.1×10^{-3}
	07PeKaRoPe [21]	6663.76–6733.43	115/1/114/0	2.0×10^{-3}	2.3×10^{-3}
	10CaSoMoPe [23]	7238.09–7917.30	332/0/332/0	8.0×10^{-4}	8.7×10^{-4}
	17KaCaKaTa [29]	7386.25–7917.30	38/0/38/0	1.0×10^{-3}	1.4×10^{-3}
	14KaKaTaPe [27]	8027.70–8060.77	13/0/13/0	1.0×10^{-3}	1.0×10^{-3}
$^{17}O^{12}C^{17}O$	98ClTeHuVa [35]	582.04–2367.48	502/0/502/0	2.5×10^{-4}	2.9×10^{-4}
(727)	80ReFlGo [34]	629.88–695.93	77/0/77/0	5.0×10^{-3}	5.9×10^{-3}
	86BrSoFr_C [52]	910.00–1106.20	242/0/242/0	2.4×10^{-5}	2.5×10^{-5}
	12LyKaJaLu [24]	1855.21–8229.20	4007/20/3987/0	1.0×10^{-3}	1.2×10^{-3}
	14ElSuMi [40]	2274.24–2366.15	69/0/69/0	3.0×10^{-6}	3.0×10^{-6}
	14BoJaLyTa [25]	3234.42–4681.07	1945/91/1854/0	1.6×10^{-4}	2.7×10^{-4}
	12JaGuLyKa [12]	3620.80–3706.53	83/0/83/0	1.0×10^{-4}	1.1×10^{-4}
	15BoJaLyTa [28]	4681.92–5295.09	1440/0/1440/0	2.1×10^{-4}	3.7×10^{-4}
	19MoKaPeTa [33]	5696.71–5823.95	40/0/40/0	1.0×10^{-3}	1.0×10^{-3}
	15JaBoLyTa [41]	5947.38–6453.43	557/0/557/0	3.0×10^{-4}	6.9×10^{-4}
	14KaCaMoKa [26]	5952.94–6932.78	552/0/552/0	1.0×10^{-3}	1.2×10^{-3}
	12VaKaHe [63]	6073.64–6459.55	370/0/300/70	2.0×10^{-3}	7.8×10^{-3}
	11VaKaHe [37]	6084.50–6151.28	116/0/96/20	2.0×10^{-3}	5.0×10^{-3}
	17KaCaKaTa [29]	7298.77–7478.96	36/0/36/0	1.0×10^{-3}	1.1×10^{-3}
	13GoHeLy [38]	8058.69–8230.61	166/0/166/0	2.0×10^{-3}	2.5×10^{-3}
	13PaLiLuLi [39]	12510.69–12570.41	51/0/51/0	3.0×10^{-3}	3.2×10^{-3}

1 3 e/f) ← (J'' 0 1 1 0 0 e/f). It seems that these transitions belong to hitherto unknown VBOs, but the upper states are not (J' 3 1 1 1 2 e/f) and (J' 3 1 1 1 3 e/f), as these assignments are in conflict with both their CDSD-296 [9] counterparts and with previous measurements [26, 41].

It is important to emphasise that, breaking away from our usual treatment, in the case of 727 we decided to add calculated lines published in 86BrSoFr [52] to the MARVEL input dataset. We did this because (a) this is one of the most accurate sources of rovibrational energy levels for 727, and (b) as mentioned in Section 2.3, the spectroscopic network of 727 can be divided into two principal components, *para* and *ortho*, that become connected by the inclusion of the accurate calculated 86BrSoFr lines into the network. To connect the two principal components, it would have also been possible to use a *magic number*, that is, a single artificial transition that connects the lowest energy levels of the *para* and *ortho* components. It is possible to check the correctness of this artificial connection of the principal components by examining the value of the lowest *ortho* energy level. The value of the (1 0 0 0 0 1 e) level in the CDSD-296 dataset is 0.734389 hc cm^{-1}, while our value in the connected network is 0.734390 hc cm^{-1}, i.e. the difference is 1×10^{-6} hc cm^{-1}, which means perfect agreement, as expected.

The original spectroscopic network assembled for 637 contained four floating components with at least 10, in fact, 14, 14, 14, and 12, energy levels. To link these larger floating components to the single principal component, we selected four artificial transitions, with an expanded uncertainty of 0.005 cm^{-1}, using rotational energy values from the CDSD-296 [9] database. In the transition file, these artificial transitions are tagged as 19CDSD. In the case of the 727 isotopologue, we found three floating components, each containing the following number of energy levels: 23, 13, and 12. We also used the energy

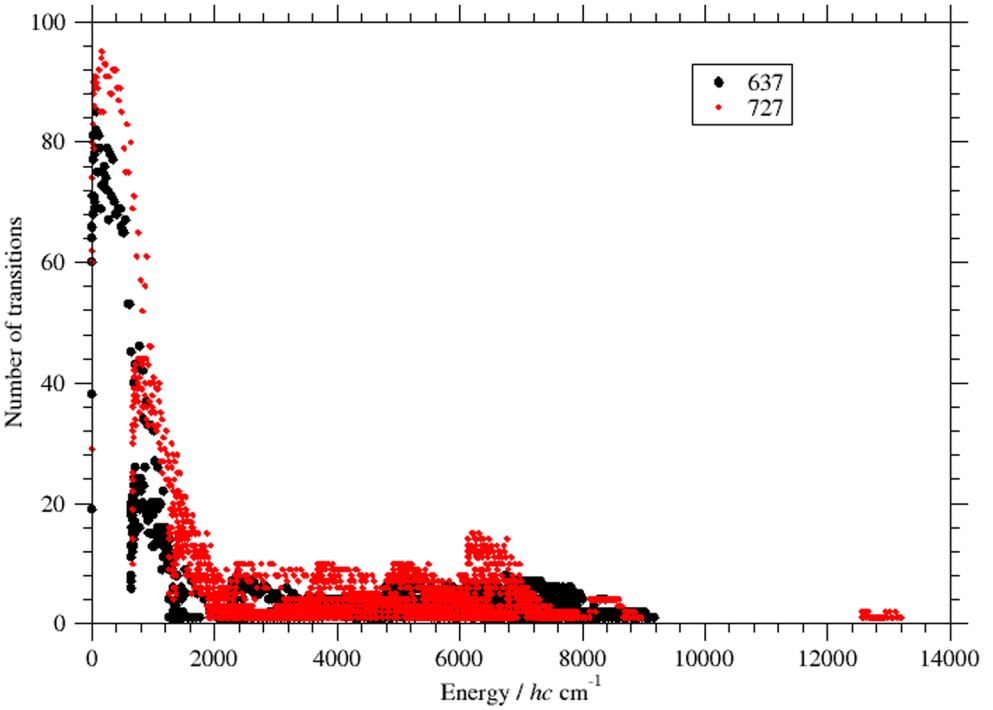

Figure 2. The number of transitions incident to each energy level versus the empirical rovibrational energy level values determined in this study for $^{16}O^{13}C^{17}O$ (637, black dots) and $^{17}O^{12}C^{17}O$ (727, red dots).

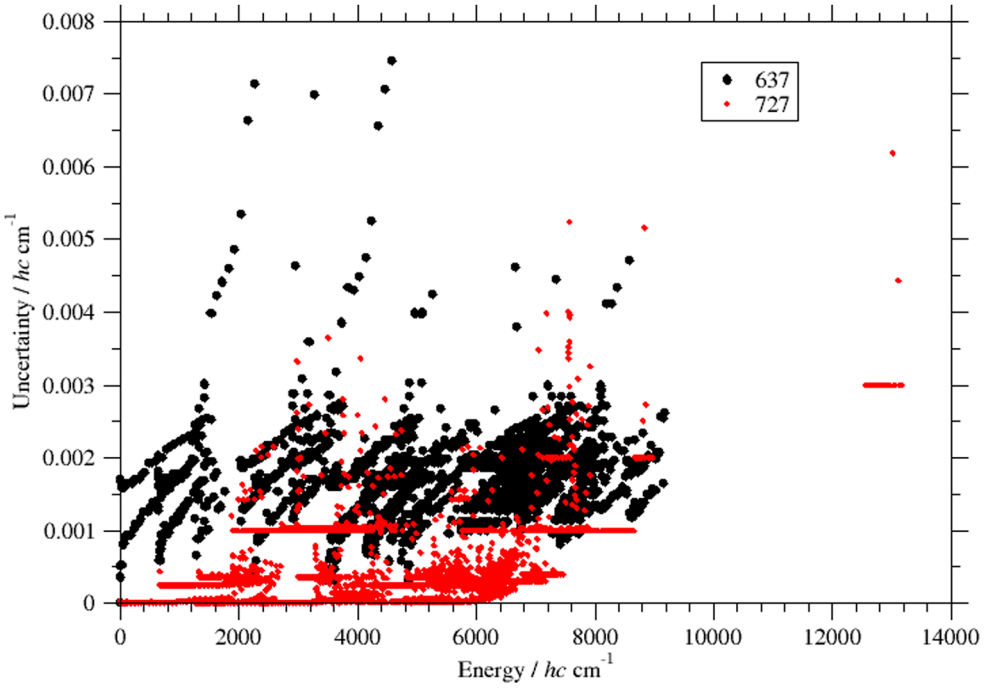

Figure 3. Empirical rovibrational energy level values determined in this study for $^{16}O^{13}C^{17}O$ (637, black dots) and $^{17}O^{12}C^{17}O$ (727, red dots) versus the energy-level uncertainties suggested by MARVEL. For 637 the smallest uncertainty is 3×10^{-4} *hc* cm^{-1}, it is for the energy level 3509.12637 *hc* cm^{-1}. For 727, the smallest uncertainty is 3×10^{-6} *hc* cm^{-1} for the energy level 2331.321624 *hc* cm^{-1}.

levels in the CDSD-296 [9] database to create the three artificial transitions, with an expanded uncertainty of 0.005 cm^{-1}, which connect these floating components to the principal components.

In what follows, comments are made on those few sources where a relatively large number of transitions had to be corrected or remained invalidated in the case of the 637 isotopologue.

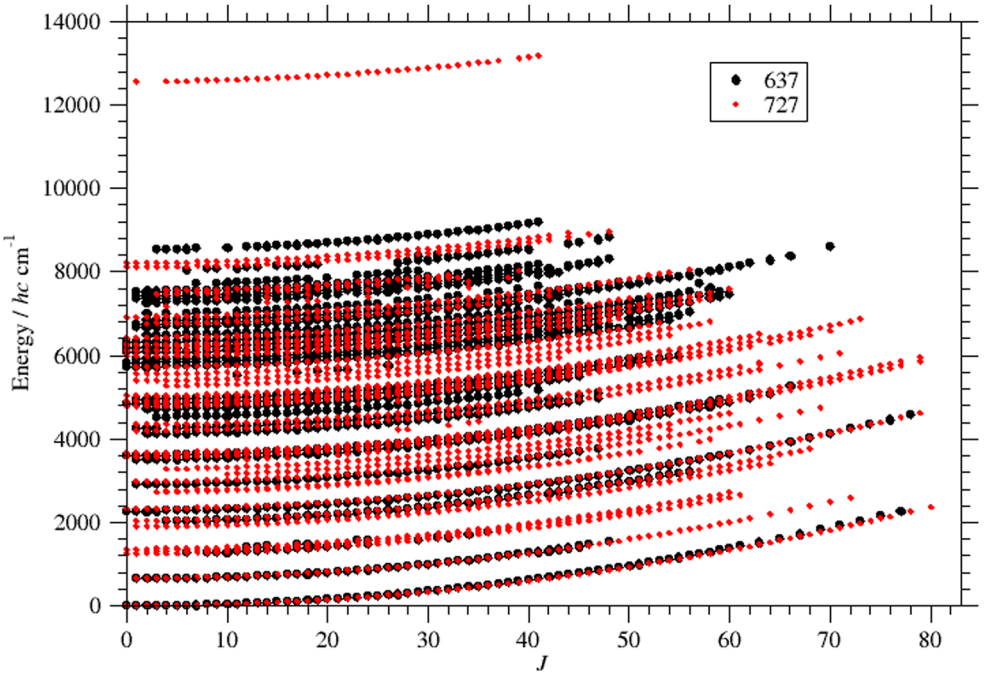

Figure 4. Empirical rovibrational energy levels determined for $^{16}O^{13}C^{17}O$ (637, black dots) and $^{12}O^{12}C^{17}O$ (727, red dots) using the MARVEL procedure versus the rotational quantum number *J*.

10CaSoMoPe [23]: We had to reassign 17 lines for 637 reported in this source to harmonise them with the corresponding measured 17KaCaKaTa [29] and calculated CDSD-296 [9] results. During the reassignment, the *J* values of the upper and lower states of these 17 lines had to be reduced by one. These lines are denoted by the tag 'relab' in the *transitions_637.txt* file of the Supplementary Material.

12LyKaJaLu [24]: 42 transitions of 727, that is more than 5% of all the transitions reported in this source, form floating components. The largest floating component contains nine energy levels.

14BoJaLyTa [25]: For 727, 91 transitions form floating components.

08PePeCa [22]: For 637, 32 transitions form floating components.

2.5. Comments on the literature sources not used

Among all the experimental sources with spectroscopic data for 637 and 727 we analysed, only the sources 99ClTeHuVa [36] and 08ToBrMiDe [64] were excluded from our MARVEL analysis. These studies focussed primarily on intensity data, no measured line-centre positions were found for the current analysis.

3. Results and discussion

3.1. Energy levels

Figure 2 shows the degree distributions, that is the number of transitions incident to each energy level, of the spectroscopic networks assembled for $^{16}O^{13}C^{17}O$ and $^{17}O^{12}C^{17}O$. The two distributions are highly similar and, just as expected [45, 65], both can be characterised as heavy-tailed, showing a power-law-like behaviour. This degree distribution means that there are a small number of quantum states, called hubs, which have a relatively large number of incident transitions. These are the most important quantum states of the two isotopologues, whose accurate experimental characterisation is especially important. It is reasonable [66] to call a quantum state a hub when more than 1% of the transitions are incident to it. This means 31/66 transitions for 636/727. As expected, hubs of both 637 and 727 belong to the ground vibrational state; however, while the 637 hubs have rotational quantum numbers $J = 15$, 21, and 20 (with 99, 95, and 94 transitions, respectively), the most frequently occurring rotational quantum numbers of the 727 hubs are $J = 14$, 13, and 9 (with 85, 82, and 81 transitions). It is less expected that despite the factor of two difference in the number of unique transitions measured for 636 and 727, the largest number of incident transitions is thus about the same for these two carbon dioxide isotopologues. Figure 2 also clearly shows that at around 13,000 $hc\,\mathrm{cm}^{-1}$ energy levels are available only for the 727 isotopologue; actually, these levels originate from the measurements reported in 13PaLiLuLi [39] (see also Table 2).

Figure 3 shows the expanded uncertainties of the empirical rovibrational energy levels determined in this study for $^{16}O^{13}C^{17}O$ and $^{17}O^{12}C^{17}O$ against the energy

level values determined through MARVEL. Clearly, the 727 data points generally show significantly lower uncertainties compared to the 637 data points, particularly at lower energy values. The majority of the points cluster below an uncertainty of 0.002 $hc\,\mathrm{cm}^{-1}$. However, some outliers for 637 extend even above 0.007 $hc\,\mathrm{cm}^{-1}$.

The empirical rovibrational energy levels determined in this study, depicted in Figure 4, have J values up to 78 and 80 for the 637 and 727 isotopologues of carbon dioxide, respectively. Each dotted curve of Figure 4 corresponds to a vibrational band, with the dots representing different J values. The energies of the vibrational band origins, defined as the lowest-energy state for a set of vibrational quantum numbers, are 18/38 for 637/727; these are listed in Table 3, whereby in more than half of the cases $J \neq 0$. As seen in Table 3, the VBOs of the 727 isotopologue are significantly more accurate than those of 637. This is due to the source 86BrSoFr [52], as its calculated transitions allow the more accurate determination of the lower VBOs.

Figure 5 gives an overview of the Fermi number, r, which is used to label the states as function of the energy of the rovibational states. Only seven energy levels have Fermi resonance number 5, for the 727 isotopologue.

3.2. Comparison with the databases CDSD-296 and Ames-2021

Figure 6 shows the absolute deviations of the rovibrational energy levels of $^{16}O^{13}C^{17}O$ between the MARVEL and the CDSD-296 [9] and Ames-2021 [8] datasets. The root-mean-square deviations of the present MARVEL and the CDSD-296 and Ames-2021 energies are 0.0018 and 0.0220 $hc\,\mathrm{cm}^{-1}$, respectively. It can also be seen from Figure 6 that there are a few MARVEL energy levels that differ from the CDSD-296 results by more than 0.01 $hc\,\mathrm{cm}^{-1}$.

To check these significant deviations, we have collected the experimentally measured transitions that determine the problematic energy levels. Table 4 contains these seven transitions, grouped by the upper energy level of the transition. As seen in Table 4, there are five different upper energy levels that are assumed to be incorrect, three of which are determined by the source 10CaSoMoPe [23] and two by 08PePeCa [22]. Unfortunately, based on the information available, it is impossible to decide whether the CDSD-296 or the experimentally measured positions are the (in)correct ones; further measurements are needed to solve this issue.

Figure 7 shows the absolute deviations of the $^{17}O^{12}C^{17}O$ rovibrational energy levels between the MARVEL and the CDSD-296 [9] and Ames-2021 [8] datasets. The root-mean-square deviations of the present MARVEL and the CDSD-296 and Ames-2021 energies are 0.0015 and 0.0218 $hc\,\mathrm{cm}^{-1}$, respectively. Clearly, the agreement is significantly better with the CDSD-296 set and there are a large number of energy levels where the agreement is better than 10^{-5} $hc\,\mathrm{cm}^{-1}$.

Table 3. Experimentally determined lowest-energy states for vibrational bands of the $^{16}O^{13}C^{17}O$ (637) and $^{17}O^{12}C^{17}O$ (727) isotopologues of carbon dioxide, obtained in this study, and their counterparts in the CDSD-296 [9] database. All energy values are in $hc\,\mathrm{cm}^{-1}$.

Isotopologue	Full label	MARVEL	CDSD-296
637	(0 0 0 0 0 1 e)	0.0000(0)	0.0000
	(1 0 1 1 0 1 e)	646.498(2)	646.5039
	(1 0 1 1 0 1 f)	646.507(2)	646.5051
	(0 0 0 0 1 1 e)	2274.088(2)	2274.0871
	(1 0 1 1 1 1 e)	2908.926(2)	2908.9288
	(0 1 0 0 1 1 e)	3608.550(2)	3608.5495
	(1 1 1 1 1 1 f)	4262.278(2)	4262.2852
	(1 1 1 1 1 1 e)	4262.287(2)	4262.2836
	(0 2 0 0 1 2 e)	4849.393(2)	4849.3921
	(0 1 0 0 2 2 e)	5738.069(2)	5738.0660
	(0 1 0 0 2 1 e)	5838.935(2)	5838.9344
	(0 3 0 0 1 3 e)	6071.574(2)	6071.5734
	(0 3 0 0 1 2 e)	6188.053(2)	6188.0507
	(0 3 0 0 1 1 e)	6318.429(2)	6318.4339
	(1 3 1 1 1 3 e)	6686.745(2)	6686.7486
	(1 3 1 1 1 3 f)	6686.749(2)	6686.7514
	(1 0 1 1 3 1 e)	7364.007(2)	7364.0104
	(1 0 1 1 3 1 f)	7364.011(2)	7364.0115
727	(0 0 0 0 0 1 e)	0.0000(0)	0.0000
	(1 0 1 1 0 1 f)	662.8007(3)	662.8022
	(1 0 1 1 0 1 e)	662.8039(4)	662.8011
	(0 1 0 0 0 2 e)	1258.235763(3)	1258.2358
	(2 0 2 2 0 1 e)	1326.7424(4)	1326.7421
	(2 0 2 2 0 1 f)	1326.7436(4)	1326.7421
	(0 1 0 0 0 1 e)	1364.940558(3)	1364.9406
	(1 1 1 1 0 2 e)	1900.990(1)	1900.9892
	(1 1 1 1 0 1 e)	2048.860(2)	2048.8583
	(0 0 0 0 1 1 e)	2330.593018(3)	2330.5930
	(1 0 1 1 1 1 e)	2981.016(1)	2981.0164
	(1 0 1 1 1 1 f)	2981.019(1)	2981.0174
	(0 1 0 0 1 2 e)	3568.4718(1)	3568.4718
	(2 0 2 2 1 1 f)	3632.591(1)	3632.5928
	(2 0 2 2 1 1 e)	3632.595(1)	3632.5928
	(0 1 0 0 1 1 e)	3672.69749(2)	3672.6976
	(1 1 1 1 1 2 e)	4198.9143(3)	4198.9140
	(1 1 1 1 1 2 f)	4198.9175(4)	4198.9156
	(1 1 1 1 1 1 e)	4344.1747(3)	4344.1749
	(1 1 1 1 1 1 f)	4344.1779(4)	4344.1766
	(0 2 0 0 1 3 e)	4787.57222(2)	4787.5722
	(2 1 2 2 1 2 f)	4835.4812(4)	4835.4804
	(2 1 2 2 1 2 e)	4835.4824(4)	4835.4804
	(0 2 0 0 1 2 e)	4901.03359(2)	4901.0337
	(0 2 0 0 1 1 e)	5039.36896(3)	5039.3689
	(1 2 1 1 1 3 e)	5402.7584(3)	5402.7586
	(1 2 1 1 1 3 f)	5402.7616(5)	5402.7607
	(1 2 1 1 1 2 e)	5555.2666(3)	5555.2669
	(1 2 1 1 1 2 f)	5555.2698(4)	5555.2689
	(1 2 1 1 1 1 e)	5724.2074(6)	5724.2070
	(1 2 1 1 1 1 f)	5724.2106(7)	5724.2093
	(0 3 0 0 1 4 e)	5988.9145(3)	5988.9128
	(0 3 0 0 1 3 e)	6122.7040(3)	6122.7045
	(0 3 0 0 1 2 e)	6249.944(1)	6249.9505
	(0 3 0 0 1 1 e)	6425.213(2)	6425.2060
	(0 0 0 0 3 1 e)	6917.819(1)	6917.8197
	(0 1 0 0 3 2 e)	8114.655(1)	8114.6578
	(0 1 0 0 3 1 e)	8215.041(1)	8215.0401

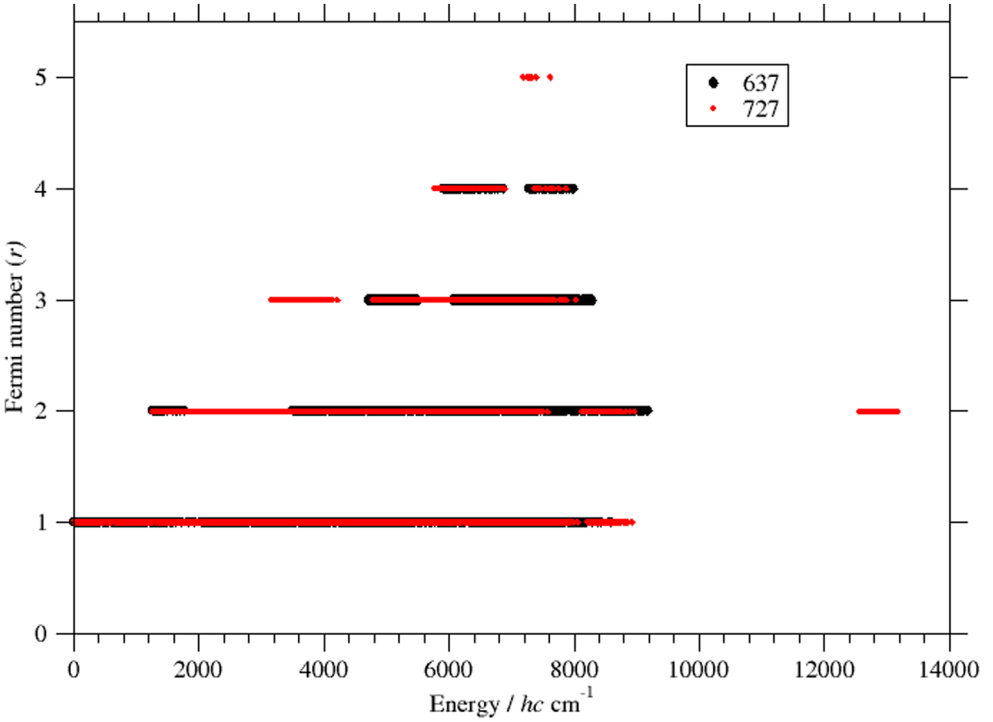

Figure 5. Fermi number *r* for each calculated energy level versus the empirical rovibrational energy levels determined in this study for $^{16}O^{13}C^{17}O$ (black dots) and $^{17}O^{12}C^{17}O$ (red dots).

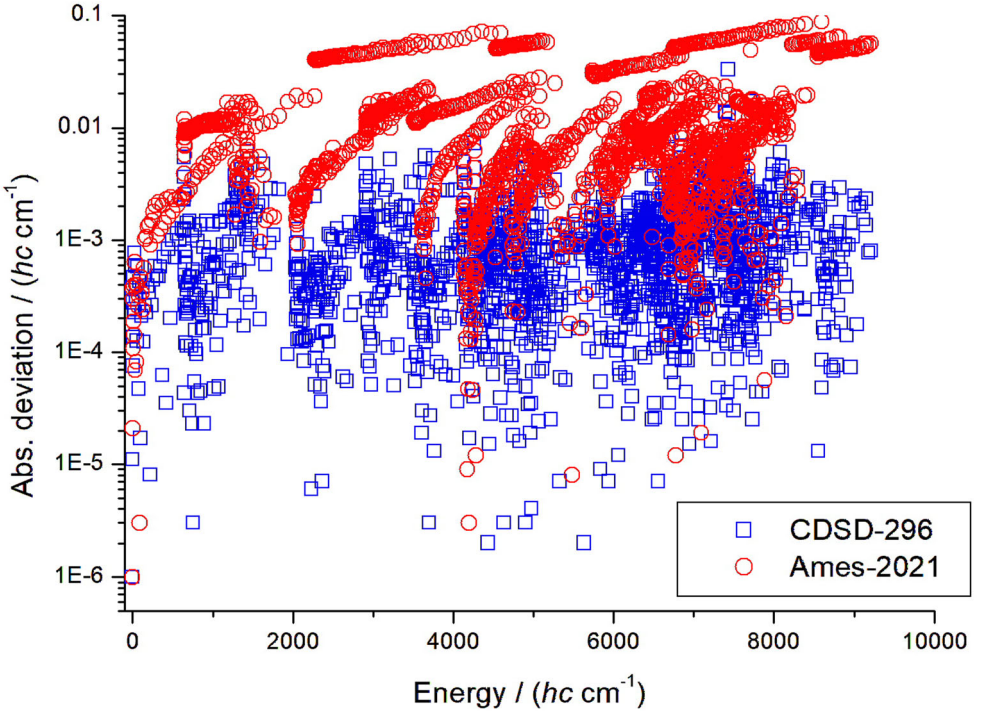

Figure 6. Comparison between the empirical rovibrational energies of the present $^{16}O^{13}C^{17}O$ dataset and those of CDSD-296 [9] (blue squares) and Ames-2021 [8] (red circles).

Table 4. Experimentally measured transitions whose deviations from their CDSD-296 [9] counterparts are larger than 0.01 hc cm^{-1} (grouped by the upper energy levels). The numbers in brackets following the measured wavenumbers show the expanded experimental uncertainty.

CDSD-296 wavenumber (cm^{-1})	Measured wavenumber (cm^{-1})	Difference (cm^{-1})	Transition	Tag
7259.486965	7259.5004(8)	0.013	(18 4 0 0 1 4 e) ← (19 0 0 0 0 1 e)	10CaSoMoPe.160
7257.807333	7257.7754(8)	0.032	(20 4 0 0 1 4 e) ← (21 0 0 0 0 1 e)	10CaSoMoPe.161
7288.845975	7288.8127(8)	0.033	(20 4 0 0 1 4 e) ← (19 0 0 0 0 1 e)	10CaSoMoPe.318
7256.960868	7256.9473(8)	0.014	(21 4 0 0 1 4 e) ← (22 0 0 0 0 1 e)	10CaSoMoPe.162
7289.512686	7289.4994(8)	0.013	(21 4 0 0 1 4 e) ← (20 0 0 0 0 1 e)	10CaSoMoPe.319
6002.125649	6002.1107(10)	0.015	(43 3 1 1 1 3 f) ← (44 0 1 1 0 1 f)	08PePeCa.491
6504.049702	6504.0658(10)	0.016	(57 1 1 1 2 1 e) ← (56 0 0 0 0 1 e)	08PePeCa.667

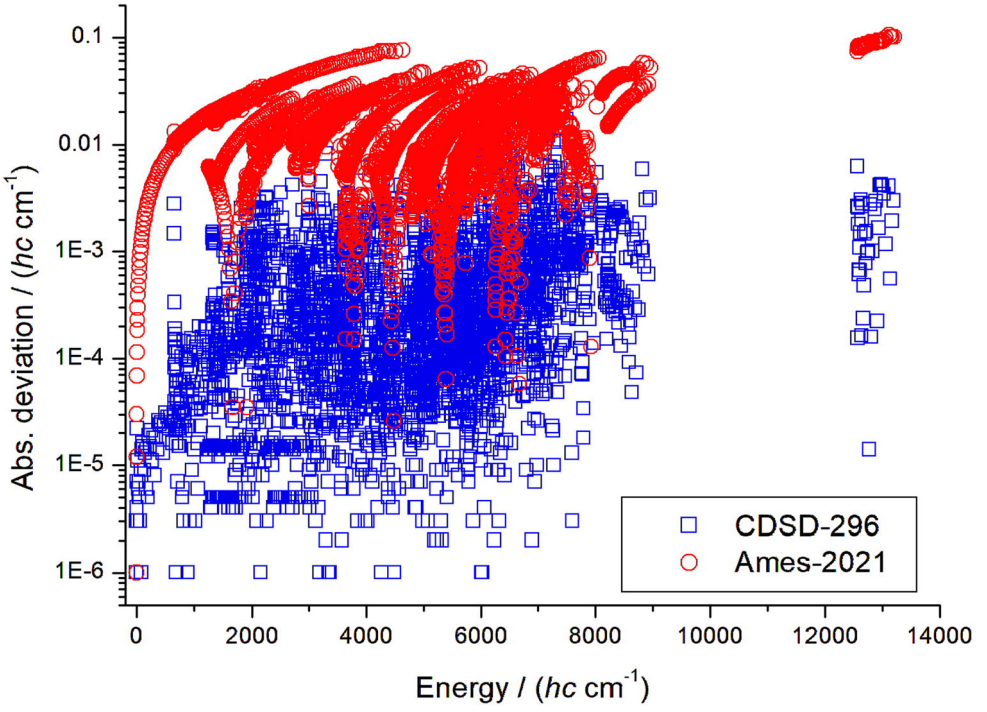

Figure 7. Comparison between the empirical rovibrational energies of the present $^{17}O^{12}C^{17}O$ dataset with those of CDSD-296 [9] (blue squares) and Ames-2021 [8] (red circles).

4. Summary and conclusions

This paper describes a comprehensive, critical, line-by-line analysis of all available measured and assigned rovibrational transitions corresponding to the ground electronic state of two minor isotopologues of carbon dioxide, $^{16}O^{13}C^{17}O$ (637) and $^{17}O^{12}C^{17}O$ (727). Our detailed and careful analysis utilises the MARVEL algorithm [42–44] and the latest version of the associated code, `MARVEL4` [47].

In total, 5053, almost exclusively experimentally measured transitions were collected from 19 literature sources for $^{16}O^{13}C^{17}O$. This dataset contains 3099 unique transitions, covering the wavenumber range 617–8061 cm^{-1}, and can be characterised by $J_{max} = 78$ and $P_{max} = 12$. This set of transitions yields 1960 empirical (MARVEL) energy levels. The average expanded (two-sigma) uncertainty of the empirical energy levels, derived from the experimental uncertainties of the transitions, is 1.75×10^{-3} hc cm^{-1}. Comparison of these energy levels with their counterparts in the CDSD-296 [9] and NASA Ames-2021 [8] databases reveals an average difference of 1.8×10^{-3} and 2.2×10^{-2} hc cm^{-1}, respectively. Thus, the agreement is significantly better with the CDSD-296 set and about the same as the internal average accuracy of the levels of the present study.

For the ninth most abundant isotopologue of carbon dioxide, $^{17}O^{12}C^{17}O$, 10,256, mostly experimentally measured transitions were collected from 16 literature sources, covering the wavenumber range 582–12,570 cm^{-1}, with $J_{max} = 80$ and $P_{max} = 17$. The dataset assembled contains 6657 transitions with unique assignments. This transition set of the 727 isotopologue yields 1960 empirical (MARVEL) energy levels with an

average expanded uncertainty of $5.53 \times 10^{-4}\,hc\,\mathrm{cm}^{-1}$. Comparison of the empirical energy levels of this study of 727 with their CDSD-296 [9] and NASA Ames-2021 [8] counterparts reveals average differences of 1.5×10^{-3} and $2.18 \times 10^{-2}\,hc\,\mathrm{cm}^{-1}$, respectively.

Disclosure statement

No potential conflict of interest was reported by the author(s).

Funding

The UK and Jordanian co-authors thank STFC for funding the UK–Jordan collaboration under the Newton Fund grant ST/T001429/1. J.T. acknowledges the support of the European Research Council (ERC) under the European Union's Horizon 2020 research and innovation programme through Advance Grant number 883830. The work of A.G.C. and F.T. received support from NKFIH (grant number K138233). This publication supports research performed within the COST Action CA21101 'Confined molecular systems: from a new generation of materials to the stars' (COSY), funded by the European Cooperation in Science and Technology (COST) and the MSCA Doctoral Network PHYMOL: 'Physics, Accuracy and Machine Learning: Towards the next-generation of Molecular Potentials'.

Data availability statement

The MARVEL input file, including all the transitions, and the MARVEL output file, with all the energy levels, are supplied as Supplementary Material to this paper. Both the measured transitions and the empirical energy levels have expanded (two-sigma) uncertainties attached to them.

ORCID

Malak H. I. Mansour http://orcid.org/0009-0006-1038-8004
Aisha B. I. Al-Iter http://orcid.org/0009-0009-2505-2476
Ala'a A. A. Azzam http://orcid.org/0000-0003-2234-355X
Jonathan Tennyson http://orcid.org/0000-0002-4994-5238
Tibor Furtenbacher http://orcid.org/0000-0002-3742-0389
Attila G. Császár http://orcid.org/0000-0001-5640-191X

References

[1] A.A.A. Azzam, D. Alatoom, B.M.J.A. Doud, M.Q.A. Shersheer, B.K.M. Almasri, C.N.M. Bader, B.O.A.K. Musleh, M.Z.J. Obaido, A.M.H.A. Khudair, A.W.M.A. Shatarat, B.I.M. Qattan, L.H.M. Hamamsy, A.O.G. Saafneh, M.N.A. ALso'ub, M.M.A. Alkhashashneh, H.O.M. Al-Zawahra, M.T.I. Ibrahim, J. Tennyson, S.N. Yurchenko, T. Furtenbacher and A.G. Császár, Sci. Data **12**, 532 (2025). doi:10.1038/s41597-025-04755-w

[2] M.T.I. Ibrahim, D. Alatoom, T. Furtenbacher, A.G. Császár, S.N. Yurchenko, A.A.A. Azzam and J. Tennyson, J. Comput. Chem. **45**, 969–984 (2024). doi:10.1002/jcc.v45.13

[3] D. Alatoom, M.T.I. Ibrahim, T. Furtenbacher, A.G. Császár, M. Alghizzawi, S.N. Yurchenko, A.A.A. Azzam and J. Tennyson, J. Comput. Chem. **45**, 2558–2573 (2024). doi:10.1002/jcc.v45.30

[4] S.A. Obaidat, A.A. Azzam, D. Alatoom, M.T.I. Ibrahim, J. Tennyson, T. Furtenbacher and A.G. Császár, J. Quant. Spectrosc. Radiat. Transfer **340**,109444(2025). doi:10.1016/j.jqsrt.2025.109444

[5] A.A.A. Azzam, J. Tennyson, S.N. Yurchenko, T. Furtenbacher and A.G. Császár, J. Comput. Chem. **46**, e27541 (2025). doi:10.1002/jcc.v46.1

[6] A.A.A. Azzam, S.A.A. Azzam, K.A.A. Aburumman, J. Tennyson, S.N. Yurchenko, A.G. Császár and T. Furtenbacher, J. Mol. Spectrosc. **405**,111947(2024). doi:10.1016/j.jms.2024.111947

[7] A.A. Azzam, J.M. AlAlawin, J. Tennyson, T. Furtenbacher and A.G. Császár, J. Quant. Spectrosc. Radiat. Transfer **343**,109485(2025). doi:10.1016/j.jqsrt.2025.109485

[8] X. Huang, D.W. Schwenke, R.S. Freedman and T.J. Lee, J. Phys. Chem. A **126**, 5940–5964 (2022). doi:10.1021/acs.jpca.2c01291.

[9] S.A. Tashkun, V.I. Perevalov, R.R. Gamache and J. Lamouroux, J. Quant. Spectrosc. Radiat. Transfer**228**, 124–131 (2019). doi:10.1016/j.jqsrt.2019.03.001

[10] I.E. Gordon, L.S. Rothman, R.J. Hargreaves, R. Hashemi, E.V. Karlovets, F.M. Skinner, E.K. Conway, C. Hill, R.V. Kochanov, Y. Tan, P. Wcisło, A.A. Finenko, K. Nelson, P.F. Bernath, M. Birk, V. Boudon, A. Campargue, K.V. Chance, A. Coustenis, B.J. Drouin, J.M. Flaud, R.R. Gamache, J.T. Hodges, D. Jacquemart, E.J. Mlawer, A.V. Nikitin, V.I. Perevalov, M. Rotger, J. Tennyson, G.C. Toon, H. Tran, V.G. Tyuterev, E.M. Adkins, A. Baker, A. Barbe, E. Canè, A.G. Császár, A. Dudaryonok, O. Egorov, A.J. Fleisher, H. Fleurbaey, A. Foltynowicz, T. Furtenbacher, J.J. Harrison, J.M. Hartmann, V.M. Horneman, X. Huang, T. Karman, J. Karns, S. Kassi, I. Kleiner, V. Kofman, F. Kwabia-Tchana, N.N. Lavrentieva, T.J. Lee, D.A. Long, A.A. Lukashevskaya, O.M. Lyulin, V.Y. Makhnev, W. Matt, S.T. Massie, M. Melosso, S.N. Mikhailenko, D. Mondelain, H.S.P. Müller, O.V. Naumenko, A. Perrin, O.L. Polyansky, E. Raddaoui, P.L. Raston, Z.D. Reed, M. Rey, C. Richard, R. Tóbiás, I. Sadiek, D.W. Schwenke, E. Starikova, K. Sung, F. Tamassia, S.A. Tashkun, J. Vander Auwera, I.A. Vasilenko, A.A. Vigasin, G.L. Villanueva, B. Vispoel, G. Wagner, A. Yachmenev and S.N. Yurchenko, J. Quant. Spectrosc. Radiat. Transfer **277**,107949(2022). doi:10.1016/j.jqsrt.2021.107949

[11] K. Calvin, D. Dasgupta, G. Krinner, A. Mukherji, P.W. Thorne, C. Trisos, J. Romero, P. Aldunce, K. Barrett, G. Blanco, W.W.L. Cheung, S. Connors, F. Denton, A. Diongue-Niang, D. Dodman, M. Garschagen, O. Geden, B. Hayward, C. Jones, F. Jotzo, T. Krug, R. Lasco, Y.-Y. Lee, V. Masson-Delmotte, M. Meinshausen, K. Mintenbeck, A. Mokssit, F.E.L. Otto, M. Pathak, A. Pirani, E. Poloczanska, H.-O. Pörtner, A. Revi, D.C. Roberts, J. Roy, A.C. Ruane, J. Skea, P.R. Shukla, R. Slade, A. Slangen, Y. Sokona, A.A. Sörensson, M. Tignor, D. van Vuuren, Y.-M. Wei, H. Winkler, P. Zhai, Z. Zommers, J.-C. Hourcade, F.X. Johnson, S. Pachauri, N.P. Simpson, C. Singh, A. Thomas, E. Totin, A. Alegría, K. Armour, B. Bednar-Friedl, K. Blok, G. Cissé,

F. Dentener, S. Eriksen, E. Fischer, G. Garner, C. Guivarch, M. Haasnoot, G. Hansen, M. Hauser, E. Hawkins, T. Hermans, R. Kopp, N. Leprince-Ringuet, J. Lewis, D. Ley, C. Ludden, L. Niamir, Z. Nicholls, S. Some, S. Szopa, B. Trewin, K.-I. van der Wijst, G. Winter, M. Witting, A. Birt and M. Ha, IPCC: 2023: Climate change 2023: Synthesis report. Contribution of working groups I, II and III to the sixth assessment report of the intergovernmental panel on climate change [core writing team, H. Lee and J. Romero (eds.)]. IPCC, Geneva, Switzerland, Tech. Rep. (2023).

[12] D. Jacquemart, F. Gueye, O.M. Lyulin, E.V. Karlovets, D. Baron and V.I. Perevalov, J. Quant. Spectrosc. Radiat. Transfer **113**, 961–975 (2012). doi:10.1016/j.jqsrt.2012.02.020

[13] M. Oosterloo, D. Höning, I.E.E. Kamp and F.F.S. van der Tak, A&A **649**, A15 (2021). doi:10.1051/0004-6361/202039664

[14] J.-Y. Mandin, J. Mol. Spectrosc. **67**, 304–321 (1977). doi:10.1016/0022-2852(77)90044-3

[15] A. Baldacci, L. Linden, V. Malathy Devi, K. Narahari Rao and B. Fridovich, J. Mol. Spectrosc. **72**, 135–142 (1978). doi:10.1016/0022-2852(78)90049-8

[16] K. Jolma, J. Mol. Spectrosc. **111**, 211–218 (1985). doi:10.1016/0022-2852(85)90002-5

[17] M.P. Esplin, H. Sakai, L.S. Rothman, G.A. Vanasse, W.M. Barowy and R.J. Huppi, Carbon dioxide line positions in the 2.8 and 4.3 micron regions at 800 Kelvin, Tech. Rep. AFGL-TR-86-0046, Utah State University (1986). https://apps.dtic.mil/sti/citations/ADA173808.

[18] J.-L. Teffo, C. Claveau and A. Valentin, J. Quant. Spectrosc. Radiat. Transfer **59**, 151–164 (1998). doi:10.1016/S0022-4073(97)00109-X

[19] Y. Ding, P. Macko, D. Romanini, V. Perevalov, S. Tashkun, J.-L. Teffo, S.-M. Hu and A. Campargue, J. Mol. Spectrosc. **226**, 146–160 (2004). doi:10.1016/j.jms.2004.03.009

[20] B.V. Perevalov, S. Kassi, D. Romanini, V.I. Perevalov, S.A. Tashkun and A. Campargue, J. Mol. Spectrosc. **238**, 241–255 (2006). doi:10.1016/j.jms.2006.05.009

[21] B.V. Perevalov, S. Kassi, D. Romanini, V.I. Perevalov, S.A. Tashkun and A. Campargue, J. Mol. Spectrosc. **241**, 90–100 (2007). doi:10.1016/j.jms.2006.11.003

[22] B.V. Perevalov, V.I. Perevalov and A. Campargue, J. Quant. Spectrosc. Radiat. Transfer **109**, 2437–2462 (2008). doi:10.1016/j.jqsrt.2008.03.010

[23] A. Campargue, K.F. Song, N. Mouton, V.I. Perevalov and S. Kassi, J. Quant. Spectrosc. Radiat. Transfer **111**, 659–674 (2010). doi:10.1016/j.jqsrt.2009.11.013

[24] O.M. Lyulin, E.V. Karlovets, D. Jacquemart, Y. Lu, A.W. Liu and V.I. Perevalov, J. Quant. Spectrosc. Radiat. Transfer **113**, 2167–2181 (2012). doi:10.1016/j.jqsrt.2012.06.028

[25] Y.G. Borkov, D. Jacquemart, O. Lyulin, S. Tashkun and V. Perevalov, J. Quant. Spectrosc. Radiat. Transfer **137**, 57–76 (2014). doi:10.1016/j.jqsrt.2013.11.008

[26] E. Karlovets, A. Campargue, D. Mondelain, S. Kassi, S. Tashkun and V. Perevalov, J. Quant. Spectrosc. Radiat. Transfer **136**, 89–107 (2014). doi:10.1016/j.jqsrt.2013.11.006

[27] E.V. Karlovets, S. Kassi, S.A. Tashkun, V.I. Perevalov and A. Campargue, J. Quant. Spectrosc. Radiat. Transfer **144**, 137–153 (2014). doi:10.1016/j.jqsrt.2014.04.001

[28] Y.G. Borkov, D. Jacquemart, O.M. Lyulin, S.A. Tashkun and V.I. Perevalov, J. Quant. Spectrosc. Radiat. Transfer **159**, 1–10 (2015). doi:10.1016/j.jqsrt.2015.02.019

[29] E. Karlovets, A. Campargue, S. Kassi, S. Tashkun and V. Perevalov, J. Quant. Spectrosc. Radiat. Transfer **191**, 75–87 (2017). doi:10.1016/j.jqsrt.2017.01.038

[30] E.V. Karlovets, P. Čermák, D. Mondelain, S. Kassi, A. Campargue, S.A. Tashkun and V.I. Perevalov, J. Quant. Spectrosc. Radiat. Transfer **217**, 73–85 (2018). doi:10.1016/j.jqsrt.2018.05.017

[31] P. Čermák, E. Karlovets, D. Mondelain, S. Kassi, V. Perevalov and A. Campargue, J. Quant. Spectrosc. Radiat. Transfer **207**, 95–103 (2018). doi:10.1016/j.jqsrt.2017.12.018

[32] E.V. Karlovets, A.D. Sidorenko, P. Čermák, D. Mondelain, S. Kassi, V.I. Perevalov and A. Campargue, J. Mol. Spectrosc. **354**, 54–59 (2018). doi:10.1016/j.jms.2018.10.003

[33] D. Mondelain, E. Karlovets, V. Perevalov, S. Tashkun and A. Campargue, J. Mol. Spectrosc. **362**, 84–89 (2019). doi:10.1016/j.jms.2019.06.004

[34] M. Reisfeld, H. Flicker and M. Goldblatt, J. Mol. Spectrosc. **82**, 411–417 (1980). doi:10.1016/0022-2852(80)90124-1

[35] C. Claveau, J.-L. Teffo, D. Hurtmans and A. Valentin, J. Mol. Spectrosc. **189**, 153–195 (1998). doi:10.1006/jmsp.1998.7546

[36] C. Claveau, J.-L. Teffo, D. Hurtmans, A. Valentin and R.R. Gamache, J. Mol. Spectrosc. **193**, 15–32 (1999). doi:10.1006/jmsp.1998.7704

[37] X. de Ghellinck d'Elseghem Vaernewijck, S. Kassi and M. Herman, Chem. Phys. Lett. **514**, 29–31 (2011). doi:10.1016/j.cplett.2011.08.025

[38] D. Golebiowski, M. Herman and O. Lyulin, Can. J. Phys. **91**, 963–965 (2013). doi:10.1139/cjp-2012-0482

[39] H. Pan, X.-F. Li, Y. Lu, A.-W. Liu, V. Perevalov, S. Tashkun and S.-M. Hu, J. Quant. Spectrosc. Radiat. Transfer **114**, 42–44 (2013). doi:10.1016/j.jqsrt.2012.08.017

[40] B.M. Elliott, K. Sung and C.E. Miller, J. Mol. Spectrosc. **304**, 1–11 (2014). doi:10.1016/j.jms.2014.08.001

[41] D. Jacquemart, Y. Borkov, O. Lyulin, S. Tashkun and V. Perevalov, J. Quant. Spectrosc. Radiat. Transfer **160**, 1–9 (2015). doi:10.1016/j.jqsrt.2015.03.016

[42] A.G. Császár, G. Czakó, T. Furtenbacher and E. Mátyus, Annu. Rep. Comput. Chem.**3**, 155–176 (2007). doi:10.1016/S1574-1400(07)03009-5

[43] T. Furtenbacher, A.G. Császár and J. Tennyson, J. Mol. Spectrosc. **245**, 115–125 (2007). doi:10.1016/j.jms.2007.07.005

[44] T. Furtenbacher and A.G. Császár, J. Quant. Spectrosc. Radiat. Transfer **113**, 929–935 (2012). doi:10.1016/j.jqsrt.2012.01.005

[45] A.G. Császár, T. Furtenbacher and P. Árendás, J. Phys. Chem. A **120**, 8949–8969 (2016). doi:10.1021/acs.jpca.6b02293

[46] R. Tóbiás, T. Furtenbacher, J. Tennyson and A.G. Császár, Phys. Chem. Chem. Phys.**21**, 3473–3495 (2019). doi:10.1039/C8CP05169K

[47] J. Tennyson, T. Furtenbacher, S.N. Yurchenko and A.G. Császár, J. Quant. Spectrosc. Radiat. Transfer **316**,108902(2024). doi:10.1016/j.jqsrt.2024.108902

[48] S.N. Yurchenko, T.M. Mellor, R.S. Freedman and J. Tennyson, Mon. Not. R. Astron. Soc. **496**, 5282–5291 (2020). doi:10.1093/mnras/staa1874

[49] J. Tennyson, S.N. Yurchenko, J. Zhang, C.A. Bowesman, R.P. Brady, J. Buldyreva, K.L. Chubb, R.R. Gamache, M.N. Gorman, E.R. Guest, C. Hill, K. Kefala, A.E. Lynas-Gray, T.M. Mellor, L.K. McKemmish, G.B. Mitev, I.I. Mizus, A. Owens, Z. Peng, A.N. Perri, M. Pezzella, O.L. Polyansky, Q. Qu, M. Semenov, O. Smola, A. Solokov, W. Somogyi, A. Upadhyay, S.O.M. Wright and N.F. Zobov, J. Quant. Spectrosc. Radiat. Transfer **326**,109083(2024). doi:10.1016/j.jqsrt.2024.109083

[50] A.G. Császár and T. Furtenbacher, J. Mol. Spectrosc. **266**, 99–103 (2011). doi:10.1016/j.jms.2011.03.031

[51] T. Furtenbacher and A.G. Császár, J. Mol. Struct. **1009**, 123–129 (2012). doi:10.1016/j.molstruc.2011.10.057

[52] L. Bradley, K. Soohoo and C. Freed, IEEE J. Quantum Electron. **22**, 234–267 (1986). doi:10.1109/JQE.1986.1072967

[53] T. Furtenbacher, R. Tóbiás, J. Tennyson, O.L. Polyansky and A.G. Császár, J. Phys. Chem. Ref. Data **49**,033101(2020). doi:10.1063/5.0008253

[54] A.G. Császár, C. Fábri, T. Szidarovszky, E. Mátyus, T. Furtenbacher and G. Czakó, Phys. Chem. Chem. Phys. **14**, 1085–1106 (2012). doi:10.1039/C1CP21830A

[55] W. Ritz, Astrophys. J. **28**, 237–243 (1908). doi:10.1086/141591

[56] G. Amat and M. Pimbert, J. Mol. Spectrosc. **16**, 278–290 (1965). doi:10.1016/0022-2852(65)90123-2

[57] R.A. McClatchey, W.S. Benedict, S.A. Clough, D.E. Burch, R.F. Calfee, K. Fox, L.S. Rothman and J.S. Garing, AFCRL atmospheric absorption line parameters compilation, Tech. Rep. AFCRL-TR-73-0096, Air Force Cambridge Research Laboratories (1983). https://modis-images.gsfc.nasa.gov/JavaHAWKS/AFCRL_AALPC.pdf.

[58] L.S. Rothman and L.D.G. Young, J. Quant. Spectrosc. Radiat. Transfer **25**, 505–524 (1981). doi:10.1016/0022-4073(81)90026-1

[59] M.P. Esplin, R.J. Huppi, H. Sakai, G.A. Vanasse and L.S. Rothman, Absorption measurements of CO_2 and H_2O at high resolution and elevated temperatures, Tech. Rep. AFGL-TR-82-0057, Utah State University (1982). https://apps.dtic.mil/sti/citations/ADA113824.

[60] R.A. Toth, L.R. Brown, C.E. Miller, V. Malathy Devi and D.C. Benner, J. Quant. Spectrosc. Radiat. Transfer **109**, 906–921 (2008). doi:10.1016/j.jqsrt.2007.12.004

[61] B. Perevalov, Le spectre d'absorption du dioxyde de carbone dans le proche infrarouge (1.4–1.7 μm): Cavity Ring Down Spectroscopy, modélisation globale et bases de données, Theses, Université Joseph-Fourier – Grenoble I (2009). https://theses.hal.science/tel-07074.

[62] A. Miani and J. Tennyson, J. Chem. Phys. **120**, 2732–2739 (2004). doi:10.1063/1.1633261

[63] X. de Ghellinck d'Elseghem Vaernewijck, S. Kassi and M. Herman, Mol. Phys. **110** (21–22), 2665–2671 (2012). doi:10.1080/00268976.2012.705346

[64] R. Toth, L. Brown, C. Miller, V. Malathy Devi and D. Benner, J. Quant. Spectrosc. Radiat. Transfer**109** (6), 906–921 (2008). doi:10.1016/j.jqsrt.2007.12.004

[65] T. Furtenbacher, P. Árendás, G. Mellau and A.G. Császár, Sci. Rep. **4**, 4654 (2014). doi:10.1038/srep04654

[66] R. Tóbiás, M.L. Diouf, F.M.J. Cozijn, W. Ubachs and A.G. Császár, Commun. Chem.**7, 34** (2024). doi:10.1038/s42004-024-01103-8